Title: Divergent influences of the locus coeruleus on migraine pathophysiology

Abbreviated title: Role of locus coeruleus on migraine biology

Marta Vila-Pueyo[1], Lauren C Strother[1], Malak Kefel[1], Peter J Goadsby[1,2] & Philip R Holland[1,*]

[1]Headache Group, Basic and Clinical Neuroscience, Institute of Psychiatry, Psychology and Neuroscience, King's College London, London SE5 9NU, UK

[2]NIHR-Wellcome Trust, King's Clinical Research Facility, King's College Hospital, London SE5 9NU, UK

***Corresponding author:**

Dr Philip R Holland

Department of Basic and Clinical Neuroscience, Institute of Psychiatry, Psychology & Neuroscience, King's College London, 125 Coldharbour Lane, London SE5 9NU, U

Telephone: +44 02078484222

Email: philip.holland@kcl.ac.uk

URL:https://kclpure.kcl.ac.uk/portal/en/persons/philip-holland(d00a4a52-9519-4bf9-aed3-a94f9729a5f8)/biography.html

Number of pages: 33

Number of figures: 6

Number of words: 213 (Abstract), 452 (Introduction), 755 (Discussion).

Keywords: Migraine; Pain; Fatigue; Locus Coeruleus.

ABSTRACT

Migraine is a common disabling neurological condition that is associated with several premonitory symptoms that can occur days before the headache onset. The most commonly reported premonitory symptom is marked fatigue that has been shown to be highly predictive of an ensuing migraine attack.

The locus coeruleus (LC) is a key nucleus involved in arousal that has also been shown to impact pain processing. It provides one of the major sources of noradrenaline to the dorsal horn of the spinal cord and neocortex**.** Given the clinical association between migraine, sleep-wake regulation and fatigue we sought to determine if LC modulation could impact migraine-related phenotypes in several validated preclinical models of migraine. To determine its role in migraine-related pain, we recorded dural nociceptive-evoked responses of neurons in the trigeminocervical complex, which receives trigeminal primary afferents from the durovascular complex. Additionally, we explored the susceptibility to cortical spreading depression initiation, the presumed underlying phenomenon of migraine aura.

Our experiments reveal a potent role for LC disruption in the differential modulation of migraine-related phenotypes, inhibiting dural-evoked activation of wide dynamic neurons in the trigeminocervical complex whilst increasing cortical spreading depression susceptibility. This highlights the potential divergent impact of LC disruption in migraine physiology, which may help explain the complex interactions between dysfunctional arousal mechanisms and migraine.

INTRODUCTION

Migraine ranks as the 2nd most common cause of years lost to disability globally [10]. Despite extensive research and clinical development, there remains a major gap in migraine treatment. To date, the majority of studies have focused on targeting migraine pain [13; 16; 37]; however, there is an increasing understanding of the importance of premonitory (prodromal) symptoms as the earliest identifiable predictors of an ensuing attack [7; 24]. While the literature on the epidemiology of premonitory symptoms is not entirely resolved, key neurological symptoms such as fatigue have emerged as highly prevalent and highly predictive attack hallmarks [12; 22; 43]. The mechanisms underlying the presence of abnormal fatigue and its relationship with migraine-related nociceptive processing remain enigmatic. Migraine is intrinsically linked with regulation of sleep-wake cycles, with sleep disruption a commonly reported migraine trigger, while sleep itself is commonly reported for attack normalisation [31]. The wake promoting locus coeruleus (LC) shows clear diurnal activity levels [30] with increased activity during arousal and almost complete inactivity during sleep. As such, we sought to explore the impact of dysregulation of the LC on migraine-related phenotypes in validated preclinical models.

A potential role for the LC in migraine pathophysiology is supported by both preclinical and clinical evidence. It is responsive to trigeminovascular activation [50; 51] and several human neuroimaging studies have highlighted altered activity and functional connectivity of the dorsal rostral pons (that contains the LC amongst other nuclei), in migraine [2; 33; 35; 44]. Functionally, the LC modulates a wide variety of networks having a key role in arousal, cognition, nociception and stress circuits [45] via descending projections to the spinal cord and ascending projections throughout the CNS. These ascending and descending projections have been shown to have divergent effects on behaviour, with descending projections largely regulating spinal nociception [27] and ascending projections involved in multiple processes including nociception, stress responses, aversive behaviours and cognition [27; 45].

Importantly, the LC may directly modulate spinal trigeminal nucleus neurons [42] and its stimulation results in α2-adrenoceptor dependent [25] cerebral hypoperfusion [23], which is a known trigger of cortical spreading depression (CSD) [49], the presumed underlying phenomenon of migraine aura [8]. In the present study, we characterised the impact of LC modulation in two validated animal models of migraine, acute dural-evoked activation of the trigeminovascular system and the threshold for the induction of CSD. First, we determined the impact of acute and chronic ablation of the LC on trigeminovascular nociceptive responses that are relevant to headache, and identified the noradrenergic receptor subtypes responsible for the observed changes. In addition, we explored the impact of chronic LC ablation on the electrical and chemical thresholds for CSD induction. Some data have been presented previously in preliminary form [53; 54].

MATERIALS AND METHODS

All experiments were conducted in accordance with the UK Home Office Animals (Scientific Procedures) Act 1986 and consistent with the ARRIVE guidelines and the guidelines of the Committee for Research and Ethical Issues of International Association for the Study of Pain (Zimmermann, 1983). Male Sprague-Dawley rats (*n* = 97, 220-380 g, Charles River, UK) were maintained and group-housed under standard conditions (12-hour light-dark cycles; lights on 07:00) with food and water available *ad libitum*. All animals were randomly assigned to experimental groups based on appropriate sample size calculations (G*Power; [19]) and all analyses were conducted by an observer blinded to the experimental grouping. To avoid confounding effects regarding the diurnal cycle, all experiments were performed between the hours of 10:00 and 15:00.

1. Chronic ablation of LC

A subset of rats (*n* = 58, 240-300 g) were injected with either 50mg/kg DSP-4 (N-(2-Chloroethyl)-N-ethyl-2-bromobenzylamine hydrochloride, Sigma, UK), a neurotoxin that initially selectively destroys noradrenergic projections and cells from the LC [40], or saline intraperitoneally 15 days before surgery. Due to the instability and light sensitivity of DSP-4, dilutions in saline were prepared immediately before injection. DSP-4 was observed to induce a characteristic general decrease in locomotor activity within the first 2 hours after injection and animals were more lethargic throughout the first 4 days and had a 16% mortality rate within the same period [48].

2. *In vivo* preparation

2.1 Common surgery

On the day of the surgery, rats were initially anesthetised with isoflurane (IsoFlo, 5%, Abbott, UK) and maintained with intravenous propofol infusion (Propoflo, 33-50 mg/kg/h, Abbott). The left femoral artery and vein were cannulated for blood pressure recordings and infusion of anaesthetic, respectively. A tracheotomy was performed to ventilate the animal with oxygen-enriched air and monitor the end-tidal CO_2 throughout the experiment to keep within physiological parameters (3.5-4.5%). A rectal probe connected to a heating pad was used to keep the body temperature constant at 36.5-37°C. Rats were placed in a stereotaxic frame and underwent one of the experimental surgical preparations and experimental procedure as detailed below.

Following each experiment, animals were euthanized by an overdose of intravenous pentobarbitone (Euthathal, 200 mg/kg, Merial, UK). When the tissue was needed for immunohistochemistry, the animals were perfused with 300ml of 0.01M cooled heparinised phosphate buffer saline (PBS), followed by 250ml of 4% paraformaldehyde in 0.01M PBS (pH 7.4). The brain and spinal cord were removed and stored for 1 hour in the same fixative and then placed in a cryoprotectant solution (30% sucrose in 0.01M PBS) for at least 48 h before being serially sectioned on a freezing cryostat.

Physiological data for all experiments were displayed and saved on a personal computer using an online data analysis system (Power 1401plus and Spike5 v8.04 software, CED, UK).

2.2 Dural-evoked trigeminal activation in the trigeminocervical complex

A parietal craniotomy provided access to the dura mater overlying the middle meningeal artery (MMA) and the area was covered in mineral oil. To access the trigeminocervical complex (TCC), a partial laminectomy of the first cervical vertebra was performed and the dura mater was opened to expose the caudal medulla. After completion of the surgery, animals were left to stabilize for at least 30 min before recording.

Stimulation of perivascular afferents of the trigeminal nerve was performed by placing a bipolar stimulating electrode on the dura mater adjacent to the MMA. Dural nociceptive neurons in the TCC were identified via electrical stimulation (8-15 V, 0.5 Hz, 0.3-0.5 ms, 20 square wave electrical pulses) of the dura mater. Stimulation parameters commonly activated Aδ-fibers with latencies between 5 – 20 ms range, and less frequently, C-fibers with latencies greater than 20 ms.

Tungsten microelectrodes (0.5–1.5 MΩ) were used to record extracellularly from neurons in the TCC activated by dural electrical stimulation and with cutaneous facial receptive fields in the ophthalmic dermatome. The signal from the recording electrode was fed via an AC preamplifier (Neurolog NL104, gain x1000), through filters (NL125, bandwidth 300Hz to 20KHz) and a 50 Hz noise eliminator (Humbug), then to a second-stage amplifier (Neurolog NL106, variable gain x20 - x90), a gated amplitude discriminator (Neurolog NL201) and an analogue-to-digital converter (Power 1401plus, CED, UK) connected to a computer where it was processed and stored (Spike5 v8.04 software, CED, UK).

When a cluster of neurons sensitive to stimulation of the ophthalmic dermatome of the trigeminal nerve was identified, it was tested for convergent input from the dura mater. Trains of 20 stimuli were delivered at 5 min intervals to assess the baseline response to dural electrical stimulation. Responses were analysed

using post-stimulus histograms with a sweep length of 100 ms and a bin width of 1 ms. When stable baseline values of the stimulus-evoked responses were achieved (average of 3 stimulation series), responses were tested for up to 60 min following physiological intervention. Following the experiment, animals were euthanized and electrolytic lesions were performed in the TCC (150 µA, 120 s) to confirm the location of the recording electrode.

2.3 Acute lesion and drug injection in the LC

Rats were placed in a stereotactic frame with the nose tilted down so that bregma was 2.33 mm below lambda. A craniotomy of approximately 2 x 2 mm was performed on the interparietal bone to gain access to the LC. A concentric bipolar tungsten microelectrode, or a four-barrelled glass micropipette was placed in the LC (anterioposterior -3.4, mediolateral -1.3, dorsoventral -6.25 mm from lambda) for electrolytic lesion (200µA, 500µs, 30Hz during 3 min) or for microinjection, respectively. After each experiment, the location of the lesion or microinjection was confirmed by cryosectioning the brainstem.

Yohimbine hydrochloride, an α2 adrenoreceptor antagonist (10 mg/ml), clonidine hydrochloride, an α2 adrenoreceptor agonist (1 or 10 mg/ml), phenylephrine hydrochloride, an α1 adrenoreceptor agonist (10 mg/ml) or Chicago Sky Blue 6B powder (2%) were dissolved in saline and injected at a volume of 210nl. Doses were chosen based on literature and preliminary studies [1; 26; 46; 55].

2.4 Superior sagittal sinus (SSS) stimulation

In animals treated with saline or DSP-4, to gain access to the superior sagittal sinus (SSS), the skull was exposed and a craniotomy of the parietal bone was performed with saline-cooled drilling from bregma to lambda. Two platinum hook electrodes were then placed on the dura mater over the SSS. Effort was taken to minimize contact between the cortex and stimulating electrodes to reduce the risk of current spread to the cortex. The area was bathed in warmed mineral oil and the animals rested for 1 hour to minimize

non-specific c-Fos protein expression. Animals were then randomly divided into two experimental groups as follows:

1. Sham controls: after the 1 hour rest period with the electrodes over the SSS, animals remained in the frame for a further 2 hours, receiving no stimulation or any other manipulation (DSP-4: *n* = 6; saline: *n* = 6).
2. Stimulation: after the 1 hour rest period with the electrodes over the SSS, animals received 2 hours of electrical stimulation (0.5 Hz, 0.5 ms duration at 20-28V; DSP-4: *n* = 6; saline: *n* = 6).

Following the experiment, animals were euthanized and perfused as described above.

2.5 Cortical spreading depression (CSD)

In animals treated with saline or DSP-4 (*n* = 14 / group), anterior to lambda, a craniotomy of approximately 2 x 2 mm was performed in each parietal bone using a saline-cooled drill and dura mater was removed. This area was used for electrical or chemical CSD induction. Posterior to bregma, a similar area was drilled in each parietal bone and dura mater was also removed. In this area, a glass pipette with a tip diameter of 10 µm filled with 3M NaCl was placed 500 µm below the cortical surface (layer 4), for cortical steady state potential recording (direct current (DC) shift). The saline filled glass pipette was coupled to a micropipette holder containing an Ag/AgCl pellet to facilitate connection to a high-impedance headstage. An Ag/AgCl reference electrode was placed subcutaneously on the neck for differential recording. The signal was fed via a DC preamplifier (Neurolog NL102, gain x1000), through filters (NL125) and a 50 Hz noise eliminator (Humbug), then to a second-stage amplifier (Neurolog NL106) and an analogue-to-digital converter (Power 1401plus, CED, UK) connected to a computer where it was processed and stored (Spike5 v8.04 software, CED, UK) [29].

Following 30 minutes of baseline recordings in the left hemisphere, the left cortex was electrically stimulated at 5-minute intervals with a bipolar electrode by increasing the electric charge (5, 12.5, 25, 50,

100, 150, 200, 250, 300, 400, 500, 600, 800, 1000, 1200 µC) until a CSD was induced. After obtaining the electrical threshold for CSD in the left hemisphere, baseline recordings were performed for 30 minutes in the right hemisphere, followed by chemical induction by placing a cotton ball soaked in 1M KCl on the cortex surface. CSDs were counted for 1 hour with KCl refreshed every 15 minutes (5 µl). Following the experiment, animals were euthanized and perfused as described above. We do not expect an ordering effect of testing CSD susceptibility on ipsi- and contralateral hemispheres in the same animal as CSDs do not propagate to and have been shown to have little effect on the contralateral hemisphere [18]. To minimize this, we conducted the electrical-induction protocol first, as it generates a single CSD wave and as such is the least disruptive to cortical function. Further, to control for a potential ordering effect, the protocol was identical between saline and DSP-4 treated rats.

3. Immunohistochemistry

Cryosectioned tissue (30 µm) spanning the TCC (trigeminal nucleus caudalis, cervical spinal cord levels C1 and C2), the LC, and the cortex, were collected in an antifreeze solution (30% ethylene glycol, 20% glycerol in 0.01M PBS) and stored at -20 °C until used.

In rats treated with DSP-4 or saline, the effectiveness of DSP-4 treatment was determined by immunoreaction to dopamine-β-hydroxylase (DBH) in the LC, cortex and TCC. Sections of the LC, cortex and TCC (*n* = 2 per animal) were washed, blocked and incubated with a mouse anti-DBH antibody (1:300, overnight at 4 °C; MAB308, Millipore, UK). Immunodetection was visualised with a fluorescent goat anti-mouse secondary antibody (1:500, 90 min at RT; Alexa Fluor 568, A11031, Thermo Fisher, UK). Sections were washed in 0.01M PBS, mounted on glass slides, cover-slipped with Vectashield® (Vector Laboratories, UK) and analysed by fluorescent microscopy. Quantification of the expression of DBH was performed by a blinded researcher in ImageJ 1.49v software by measuring the percentage of the area stained, adjusting the same threshold for all the images, and the mean for each animal was calculated (*n*

= 2 sections per animal, bilateral average). Values are expressed as the percentage loss of DBH staining. Saline-treated controls were considered to have 100% staining.

In rats where the SSS was stimulated, neuronal activation of the TCC was assessed by detecting the immunoreactivity to c-Fos in the TCC. Sections of the TCC (*n* = 12 per animal) were washed, blocked and incubated with a rabbit anti-c-Fos antibody (1:10000, overnight at 4 °C; ABE457, Millipore). Immunodetection was achieved with a goat anti-rabbit biotinylated secondary antibody (1:500, 90 min at RT; BA-1000, Vector Laboratories), followed by an ABC solution amplification (1:200, 30 min at RT; ABC Elite Kit, Vector Laboratories) and a colorimetric reaction with 3,3'-diaminobenzidine (DAB) Peroxidase Substrate Kit (1:50, 1-5 min at RT; SK-4100, Vector Laboratories). Sections were washed in 0.01M PBS, mounted on glass slides, dehydrated and cover-slipped with DPX (Sigma, UK). The expression of c-Fos was identified by a blinded researcher via the identification of c-Fos-immunoreactive nuclei that were clearly distinguishable from the background level. Quantification of the expression of c-Fos in the TCC (*laminae* I, II and V) was performed by two independent counters using an optical light microscope. Values are expressed as the median and interquartile ranges per animal.

4. Statistical Analysis

Statistical analysis of raw data was performed using IBM SPSS 22.0 software and graphs were plotted with SigmaPlot 12.5 software. For each study, *n* was chosen to obtain a statistical power of 80-90% and analyses of power were performed with G*Power software [19]. Regarding CSD experiments, animals were included in the analysis only if data from both electrical and chemical stimulation were obtained. For the electrical stimulation, a threshold corresponding to the lowest current needed to induce a CSD was determined for each animal. For chemical stimulation, the number of CSDs where the cortical steady state potential was altered by at least 5mV were counted over one hour.

For CSD experiments and immunohistochemistry, we first tested for normality using the Kolmogorov-Smirnov test. If data were normally distributed, an independent Student's *t* test was used for comparison (data expressed as mean ± SEM). If data were not normally distributed, we used Kruskal-Wallis test with Monte Carlo exact test post-hoc correction (CI of 95%) and Mann Whitney *U* test for comparison with Bonferroni post-hoc correction (data expressed as a median with interquartile range).

For TCC recordings, data collected of Aδ-fiber activation represent the normalized data for the number of cells firing over a 10 ms period in the region 5-20 ms post-stimulation over 20 sweeps and is expressed as mean ± SEM. We first analysed if there was a significant effect over time in the raw data by using an ANOVA for repeated measures with Bonferroni post-hoc correction for multiple comparisons; if Mauchly's test of sphericity was violated, appropriate corrections to the degrees of freedom were made according to Greenhouse-Geisser [20]. If the ANOVA for repeated measures was significant, we proceeded to conduct post-hoc analyses. For post-hoc analyses, we first compared the similarity of baseline responses across groups. If baseline responses were not different, we compared the effect of the acute LC lesion or the yohimbine, clonidine or phenylephrine microinjection in the LC at each time point (30 and 60 min post-lesion; 1, 5, 15, 30, 45 and 60 min post-injection) with the control group (electrode placed in the LC or saline injection). Data was plotted as percentage of the mean of the three baselines obtained either before lesioning or injecting in the LC (normalized data). Animals were only included in the analysis if lesions or microinjections were performed in the LC.

RESULTS

Locus Coeruleus modulation

We applied three strategies for modulating the LC. First, to determine the impact of LC disruption we electrolytically lesioned the LC. Second, to model a more chronic depletion of LC noradrenergic fibres we utilised DSP-4, a toxin that is known to ablate selectively LC noradrenergic neurons [40] due to its uptake via the noradrenaline transporter. Finally, we explored the impact of acute pharmacological modulation of the LC to characterise potential underlying receptor mechanisms.

1. Acute disruption of the LC inhibits dural-evoked trigeminovascular activation

To assess the impact of disrupted LC signalling, we electrolytically lesioned the LC in anesthetised rats and monitored the impact of LC disruption on dural-evoked trigeminovascular activation in the trigeminocervical complex (TCC), using *in vivo* extracellular electrophysiology that is a well-established preclinical model of migraine-related nociceptive processing. As illustrated in **Figure 1A**, electrical stimulation of the perivascular afferents of the trigeminal nerve results in activation of 2nd order ascending projections from the TCC that can be recorded *in vivo* (**Figure 1B**).

Following the establishment of stable dural-evoked wide dynamic range neuronal responses, a concentric bipolar electrode was lowered into the LC in agreement with the atlas of Paxinos and Watson [38]. Placement of the electrode alone without stimulation induced a stable non-significant decrease of TCC dural-evoked neuronal activation (72 ± 11%; $t_{(5)}$ = 1.93, p = 0.112; **Figure 1C**). Subsequent electrolytic lesioning of the LC (pulses of 200 µA, 30Hz, 500µs during 3 min) resulted in a significant reduction in dural-evoked neuronal activation ($F_{6,90}$ = 4.361, p = 0.001), reaching its maximum at 60 minutes post lesion (42 ± 11%; $t_{(5)}$= 3.24, p = 0.023; **Figure 1C**), indicating a decrease in dural-evoked trigeminal activation. There were no significant differences in baseline spontaneous firing throughout the entire experiment,

suggesting the LC effects were nociceptive specific ($F_{11,110}$ = 0.693, p = 0.74). Animals were only included in the analysis if anatomical lesions were located in the LC.

2. Chronic disruption of the locus coeruleus with DSP-4

Given the anti-nociceptive effect of acute LC disruption and the previously reported anti- and pro-nociceptive effects of LC activation [15; 27], we considered that electrolytic lesioning of the LC may initially result in acute activation of the LC and increased noradrenergic signalling at its terminals. Therefore, to confirm the anti-nociceptive effect of LC disruption on dural-evoked trigeminovascular activation, we sought to chronically ablate LC noradrenergic neurons.

Two weeks following a single intraperitoneal injection of DSP-4 (50mg/kg), a well-established selective toxin for LC noradrenergic neurons that acts via noradrenaline transporter uptake mechanisms [40], we observed a significant reduction in noradrenergic neurons in the LC as identified by decreased dopamine-β-hydroxylase (DBH) immunoreactivity, compared to saline treated rats (n = 25 / group, 54 ± 5% reduction; $t_{(48)}$ = 6.32, $p \leq 0.0001$; **Figure 2A-B**). We also observed a significant reduction in DBH immunoreactive processes, most likely as a result of a loss of LC projection neurons in the cortex (n = 4 / group, 92.9 ± 3.5% reduction; $t_{(6)}$ = 14.15, $p \leq 0.0001$) and upper spinal cord (n = 4 / group, 90.2 ± 4.3% reduction; $t_{(6)}$ = 2.58, p = 0.043) when comparing DSP-4 to saline treated rats.

3. Chronic disruption of the LC inhibits dural-evoked trigeminovascular activation

Animals randomly assigned to receive either saline or DSP-4 (n = 12 each) were further subjected to sham or electrical stimulation (n = 6 per group) of the SSS to induce dural-evoked nociceptive activation of the trigeminovascular system (**Figure 2C**). Neuronal activation was then analysed by immunohistochemical detection of the marker of neuronal activation c-Fos within the dorsal horn of the TCC (**Figure 2D**).

Electrical stimulation of the SSS in saline treated animals induced a significant four-fold increase in neuronal activation in the TCC compared to sham treated rats (U = 0, p = 0.006, **Figure 2E**). However, in animals receiving DSP-4, where the LC was chronically disrupted, stimulation of the SSS failed to induce an increase in neuronal activation, showing similar levels of c-Fos expression as sham animals (U = 7, p = 0.144, **Figure 2E**). Thus, both acute lesioning and chronic ablation of the LC inhibits dural-evoked trigeminovascular activation at the level of the TCC.

4. α2-adrenoceptors-dependent inhibition of LC activity decreases dural-evoked trigeminovascular activation

Given our demonstration of the anti-nociceptive effects of acute and chronic disruption of the LC, we next sought to explore the impact of its pharmacological modulation through adrenoceptors using *in vivo* electrophysiology of dural-evoked trigeminovascular activation in the TCC combined with local microinjection into the LC.

In agreement with an inhibitory action on LC activity, the microinjection of the α2-adrenoceptor agonist clonidine in the LC significantly inhibited TCC activation in a dose-dependent manner ($F_{4.45,66.8}$ = 12.96, $p \leq$ 0.0001, **Figure 3A**), reaching a significant decrease at 30 minutes after injection of the lowest concentration (1mg/ml, $t_{(12)}$ = -2.72, p = 0.019) and at 5 minutes after injection of the highest concentration (10mg/ml, $t_{(9)}$ = -7.56, $p \leq$ 0.0001). An effect that was blocked when pre-treating with the α2-adrenoceptor antagonist yohimbine ($F_{11,77}$ = 0.88, p = 0.561, **Figure 3A**). Yohimbine alone microinjected in the LC did not have an effect on dural-evoked responses in the TCC ($F_{11,110}$ = 0.44, p = 0.94, **Figure 3B**). There were no significant differences in baseline spontaneous firing throughout the entire experiment, suggesting the LC effects were nociceptive specific ($F_{11,220}$ = 0.92, p = 0.518).

5. LC modulates dural-evoked trigeminovascular activation through α1-adrenoceptors

Given the inhibitory actions of α2-adrenoceptor activation and disruption of the LC, we sought to explore the impact of modulation of LC α1-adrenoceptors that has previously been reported to be pro-nociceptive [39]. Microinjection of the α1-adrenoceptor agonist phenylephrine into the LC resulted in an acute reduction (81 ± 5%, $t_{(10)}$ = -2.54, p = 0.029) in dural-evoked TCC neuronal activation that transitioned to increased dural-evoked TCC neuronal activation (118 ± 8%, $t_{(10)}$ = 3.01, p = 0.013, **Figure 3C**) over the one hour recording window. This is in agreement with a prolonged facilitation of nociceptive responses demonstrated by others [39]. There were no significant differences in baseline spontaneous firing throughout the entire experiment, suggesting the LC effects were nociceptive specific ($F_{1.49,14.89}$ = 1.68, p = 0.105).

6. Chronic disruption of the LC increases susceptibility to cortical spreading depression

Given the impact of LC disruption on dural-evoked trigeminovascular activation, its previously identified role in cortical blood flow regulation [23] and the fact that it provides the only source of neocortical noradrenaline [5; 32; 41], we sought to explore the effect of LC disruption on cortical spreading depression (CSD), the presumed underlying phenomenon of migraine aura [3; 4; 52].

A separate randomly assigned cohort of rats were injected with either saline or DSP-4 (n = 25) and studied to measure their CSD susceptibility. CSD can be induced with several methods; the most robust methods being electrical and chemical stimulation. Electrical stimulation allows the determination of an individual CSD threshold, while chemical stimulation determines the number of CSDs that occur after the application of the stimulus. To reduce the number of animals used and in accordance with previous studies [28], we used the electrical method to determine the CSD threshold in the left hemisphere and subsequently the chemical method to determine the number of CSDs that occurred in response to repetitive KCl application over the right hemisphere (**Figure 4D**).

Chronic disruption of the LC via DSP-4 treatment resulted in a significant decrease in the threshold required to induce CSD when compared to saline treated rats, from 209 ± 58 μC to 43 ± 7 μC (U = 43, p = 0.036), indicating an increased susceptibility to CSD initiation (**Figure 4A-C**). In agreement with an increased susceptibility to CSD, application of 1M KCl over the cortex in DSP-4 treated rats resulted in a significant increase in the number of CSDs recorded over the one hour period from 13 ± 2 to 20 ± 2 ($t_{(23)}$ = -2.5, p = 0.018, **Figure 4E-G**), that was more prominent in the final 30 minutes of the recording (**Supplementary Figure 1**).

DISCUSSION

Our experiments reveal a potent role for LC dysregulation in the modulation of dural-evoked trigeminovascular activation in the TCC and the susceptibility to CSD, the presumed underlying mechanism of migraine aura. Using two different validated preclinical models for migraine, we have identified that LC disruption decreases TCC activation to durovascular nociceptive stimulation. Importantly, activation of the LC has demonstrated divergent effects on pain, with both anti-and pro-nociceptive effects [15; 27]. To confirm that it was reduced LC signalling that was responsible for the observed anti-nociceptive effects, we chronically ablated LC noradrenergic projections and recorded TCC dural-evoked responses two weeks later.

The observed decrease in trigeminovascular activation was mimicked by the α2-adrenoceptor agonist clonidine that has been shown to inhibit LC neuronal activity [17; 34], suggesting that acute and chronic reductions in LC derived noradrenergic signalling is antinociceptive at the level of the TCC. This is further supported by the facilitation of TCC dural-evoked trigeminal activation by the α1-adrenoceptor agonist phenylephrine that has previously been shown to be pro-nociceptive and excites LC neurons [36; 39]. Importantly, there was no significant alteration of background trigeminovascular activity suggesting that the observed effects were nociceptive specific. As such, we hypothesise that the LC may be a key nucleus involved in sleep-induced migraine attack normalisation. Locus coeruleus activity is lowest during sleep [30] and as such sleep-induced reductions in LC activity may act to inhibit aberrant nociceptive-specific trigeminal activity at the level of the TCC and reduce the sensory input to the perturbed migraine brain [3]. Correspondingly, it is known that TCC neuronal excitability increases in migraine patients as they near the next attack [47]. As such, it could be hypothesised that decreasing LC activity would act to normalise this developing excitability with subsequent impacts on LC arousal related mechanisms (**Figure 5**), leading to abnormal fatigue [21; 22]. As discussed, the LC has been shown to have divergent effects on spinal nociception, with both pro- and anti-nociceptive effects [15; 27]. This is likely due to the heterogeneous

population of LC neuronal projections with both descending and ascending pathways [27]. As we recorded wide dynamic range neuronal responses in the TCC as a surrogate marker of trigeminal mediated nociceptive activation, we are unable to determine if LC ablation or pharmacological modulation impacts pain behaviours in conscious freely behaving animals. Future studies should determine the specific effects of targeting ascending and descending pathways individually in such conditions.

Given that LC ablation with DSP-4 depleted cortical and spinal noradrenergic expression, we hypothesised that loss of ascending noradrenergic signalling to the cortex would render it hyper-excitable and decrease the threshold for CSD. This is in agreement with the ability of LC stimulation to alter cortical blood flow [23]. Chronic ablation of the LC resulted in a significant decrease in the electrical threshold required to induce CSD and a significant increase in the number of CSD's induced by repetitive KCl application to the cortex. Our results suggest that dysregulation of the LC may increase the likelihood of CSD induction and migraine aura. This is in agreement with a previous study where indirect activation of the LC via vagus nerve stimulation [11; 14] decreased the susceptibility to CSD [9]. Importantly, there remains some controversy over the impact of LC ablation on cortical extracellular noradrenaline levels [40], as DSP-4 treated animals have been shown to have unchanged or increased extracellular concentrations in the cortex despite decreased tissue levels [6]. This increase is thought to result from passive spread from non-coerulean sources combined with a lack of local noradrenaline uptake. As such, local tissue decreases may occur in the presence of an increased extracellular concentration of noradrenaline that may augment CSD susceptibility.

Taken together, our results show a direct involvement of the LC in the regulation of migraine pathophysiology, whereby dysfunctional LC signalling may alter attack susceptibility. Although the existing models cannot reproduce the intricate modulation that the LC exerts throughout the CNS, we determined that decreased spinal LC noradrenergic signalling inhibits dural-evoked trigeminal activation at the level of the TCC. This highlights a potential anti-nociceptive action of LC inhibition on migraine-related pain.

Conversely, decreased cortical LC noradrenergic signalling reduced the threshold for CSD induction, suggesting the potential for LC dysregulation to impact the occurrence of migraine aura. Our results highlight the LC and its noradrenergic projections as a key nucleus in the regulation of migraine pathophysiology. Given the arousal-related functions of the LC, its role in stress regulation and cognition, we further predict that the dysfunctional LC signalling may in part underlie migraine-associated symptoms including abnormal fatigue.

ACKNOWLEDGEMENTS

The study received support from the Wellcome Trust (grant number 104033). The Medical Research Council (grant number MR/P006264/1). The FP7 program EUROHEADPAIN (grant agreement no: 602633) of the European Union. and the International Headache Society. MV-P was an International Headache Society Fellow.

Conflict of interest: MV-P, LCS & MK declare no competing financial interests. PJG reports, unrelated to the current project, grants and personal fees from Allergan, Amgen, and Eli-Lilly and Company; and personal fees from Akita Biomedical, Alder Biopharmaceuticals, Cipla Ltd, Dr Reddy's Laboratories, eNeura, Electrocore LLC, Novartis, Pfizer Inc, Quest Diagnostics, Scion, Teva Pharmaceuticals, Trigemina Inc., Scion; and personal fees from MedicoLegal work, Journal Watch, Up-to-Date, Massachusetts Medical Society, Oxford University Press; and in addition, Dr. Goadsby has a patent Magnetic stimulation for headache assigned to eNeura without fee. PRH reports, unrelated to the current project, honoraria for educational and advisory purposes from Allergan, Novartis and TEVA as well as research funding from Amgen and Eli-Lilly.

REFERENCES

[1] Adams LM, Foote SL. Effects of locally infused pharmacological agents on spontaneous and sensory-evoked activity of locus coeruleus neurons. Brain Res Bull 1988;21(3):395-400.

[2] Afridi SK, Giffin NJ, Kaube H, Friston KJ, Ward NS, Frackowiak RS, Goadsby PJ. A positron emission tomographic study in spontaneous migraine. Arch Neurol 2005;62(8):1270-1275.

[3] Akerman S, Holland PR, Goadsby PJ. Diencephalic and brainstem mechanisms in migraine. Nat Rev Neurosci 2011;12(10):570-584.

[4] Ayata C, Jin H, Kudo C, Dalkara T, Moskowitz MA. Suppression of cortical spreading depression in migraine prophylaxis. Ann Neurol 2006;59(4):652-661.

[5] Berridge CW, Waterhouse BD. The locus coeruleus-noradrenergic system: modulation of behavioral state and state-dependent cognitive processes. Brain Res Brain Res Rev 2003;42(1):33-84.

[6] Bortolozzi A, Artigas F. Control of 5-hydroxytryptamine release in the dorsal raphe nucleus by the noradrenergic system in rat brain. Role of alpha-adrenoceptors. Neuropsychopharmacology 2003;28(3):421-434.

[7] Burstein R, Noseda R, Borsook D. Migraine: multiple processes, complex pathophysiology. J Neurosci 2015;35(17):6619-6629.

[8] Charles AC, Baca SM. Cortical spreading depression and migraine. Nat Rev Neurol 2013;9(11):637-644.

[9] Chen SP, Ay I, de Morais AL, Qin T, Zheng Y, Sadeghian H, Oka F, Simon B, Eikermann-Haerter K, Ayata C. Vagus nerve stimulation inhibits cortical spreading depression. Pain 2016;157(4):797-805.

[10] Collaborators GBDCoD. Global, regional, and national age-sex specific mortality for 264 causes of death, 1980-2016: a systematic analysis for the Global Burden of Disease Study 2016. Lancet 2017;390(10100):1151-1210.

[11] Cunningham JT, Mifflin SW, Gould GG, Frazer A. Induction of c-Fos and DeltaFosB immunoreactivity in rat brain by Vagal nerve stimulation. Neuropsychopharmacology 2008;33(8):1884-1895.

[12] Cuvellier JC, Mars A, Vallee L. The prevalence of premonitory symptoms in paediatric migraine: a questionnaire study in 103 children and adolescents. Cephalalgia 2009;29(11):1197-1201.

[13] Diener HC, Charles A, Goadsby PJ, Holle D. New therapeutic approaches for the prevention and treatment of migraine. Lancet Neurol 2015;14(10):1010-1022.

[14] Dorr AE, Debonnel G. Effect of vagus nerve stimulation on serotonergic and noradrenergic transmission. J Pharmacol Exp Ther 2006;318(2):890-898.

[15] Drummond PD. A possible role of the locus coeruleus in complex regional pain syndrome. Front Integr Neurosci 2012;6:104.

[16] Edvinsson L, Haanes KA, Warfvinge K, Krause DN. CGRP as the target of new migraine therapies - successful translation from bench to clinic. Nat Rev Neurol 2018;14(6):338-350.

[17] Engberg G, Eriksson E. Effects of alpha 2-adrenoceptor agonists on locus coeruleus firing rate and brain noradrenaline turnover in N-ethoxycarbonyl-2-ethoxy-1,2-dihydroquinoline (EEDQ)-treated rats. Naunyn Schmiedebergs Arch Pharmacol 1991;343(5):472-477.

[18] Faraguna U, Nelson A, Vyazovskiy VV, Cirelli C, Tononi G. Unilateral cortical spreading depression affects sleep need and induces molecular and electrophysiological signs of synaptic potentiation in vivo. Cereb Cortex 2010;20(12):2939-2947.

[19] Faul F, Erdfelder E, Lang AG, Buchner A. G*Power 3: a flexible statistical power analysis program for the social, behavioral, and biomedical sciences. Behav Res Methods 2007;39(2):175-191.

[20] Field A. Discovering statistics using SPSS. London: SAGE publications, 2005.

[21] Giffin NJ, Lipton RB, Silberstein SD, Olesen J, Goadsby PJ. The migraine postdrome: An electronic diary study. Neurology 2016;87(3):309-313.

[22] Giffin NJ, Ruggiero L, Lipton RB, Silberstein SD, Tvedskov JF, Olesen J, Altman J, Goadsby PJ, Macrae A. Premonitory symptoms in migraine: an electronic diary study. Neurology 2003;60(6):935-940.

[23] Goadsby PJ, Duckworth JW. Low frequency stimulation of the locus coeruleus reduces regional cerebral blood flow in the spinalized cat. Brain Res 1989;476(1):71-77.

[24] Goadsby PJ, Holland PR, Martins-Oliveira M, Hoffmann J, Schankin C, Akerman S. Pathophysiology of Migraine: A Disorder of Sensory Processing. Physiol Rev 2017;97(2):553-622.

[25] Goadsby PJ, Lambert GA, Lance JW. The mechanism of cerebrovascular vasoconstriction in response to locus coeruleus stimulation. Brain Res 1985;326(2):213-217.

[26] Hayashida K, Parker RA, Eisenach JC. Activation of glutamate transporters in the locus coeruleus paradoxically activates descending inhibition in rats. Brain Res 2010;1317:80-86.

[27] Hickey L, Li Y, Fyson SJ, Watson TC, Perrins R, Hewinson J, Teschemacher AG, Furue H, Lumb BM, Pickering AE. Optoactivation of locus ceruleus neurons evokes bidirectional changes in thermal nociception in rats. J Neurosci 2014;34(12):4148-4160.

[28] Hoffmann U, Sukhotinsky I, Eikermann-Haerter K, Ayata C. Glucose modulation of spreading depression susceptibility. J Cereb Blood Flow Metab 2013;33(2):191-195.

[29] Holland PR, Akerman S, Andreou AP, Karsan N, Wemmie JA, Goadsby PJ. Acid-sensing ion channel 1: a novel therapeutic target for migraine with aura. Ann Neurol 2012;72(4):559-563.

[30] Jacobs BL. Single unit activity of locus coeruleus neurons in behaving animals. Prog Neurobiol 1986;27(2):183-194.

[31] Kelman L. The triggers or precipitants of the acute migraine attack. Cephalalgia 2007;27(5):394-402.

[32] Levitt P, Moore RY. Noradrenaline neuron innervation of the neocortex in the rat. Brain Res 1978;139(2):219-231.

[33] Maniyar FH, Sprenger T, Monteith T, Schankin C, Goadsby PJ. Brain activations in the premonitory phase of nitroglycerin-triggered migraine attacks. Brain 2014;137(Pt 1):232-241.

[34] Marwaha J, Kehne JH, Commissaris RL, Lakoski J, Shaw W, Davis M. Spinal clonidine inhibits neural firing in locus coeruleus. Brain Res 1983;276(2):379-383.

[35] Moulton EA, Becerra L, Johnson A, Burstein R, Borsook D. Altered hypothalamic functional connectivity with autonomic circuits and the locus coeruleus in migraine. PLoS One 2014;9(4):e95508.

[36] Nakamura S, Sakaguchi T, Kimura F, Aoki F. The role of alpha 1-adrenoceptor-mediated collateral excitation in the regulation of the electrical activity of locus coeruleus neurons. Neuroscience 1988;27(3):921-929.

[37] Ong JJY, Wei DY, Goadsby PJ. Recent Advances in Pharmacotherapy for Migraine Prevention: From Pathophysiology to New Drugs. Drugs 2018;78(4):411-437.

[38] Paxinos GW, Charles. The rat brain in stereotaxic coordinates, 5th edition: Elsevier, 2005.

[39] Pertovaara A. Noradrenergic pain modulation. Prog Neurobiol 2006;80(2):53-83.

[40] Ross SB, Stenfors C. DSP4, a selective neurotoxin for the locus coeruleus noradrenergic system. A review of its mode of action. Neurotox Res 2015;27(1):15-30.

[41] Samuels ER, Szabadi E. Functional neuroanatomy of the noradrenergic locus coeruleus: its roles in the regulation of arousal and autonomic function part I: principles of functional organisation. Curr Neuropharmacol 2008;6(3):235-253.

[42] Sasa M, Takaori S. Influence of the locus coeruleus on transmission in the spinal trigeminal nucleus neurons. Brain Res 1973;55(1):203-208.

[43] Schoonman GG, Evers DJ, Terwindt GM, van Dijk JG, Ferrari MD. The prevalence of premonitory symptoms in migraine: a questionnaire study in 461 patients. Cephalalgia 2006;26(10):1209-1213.

[44] Schulte LH, May A. The migraine generator revisited: continuous scanning of the migraine cycle over 30 days and three spontaneous attacks. Brain 2016;139(Pt 7):1987-1993.

[45] Schwarz LA, Luo L. Organization of the locus coeruleus-norepinephrine system. Curr Biol 2015;25(21):R1051-1056.

[46] Shelkar GP, Gakare SG, Chakraborty S, Dravid SM, Ugale RR. Interactions of nitric oxide with alpha2 - adrenoceptors within the locus coeruleus underlie the facilitation of inhibitory avoidance memory by agmatine. Br J Pharmacol 2016;173(17):2589-2599.

[47] Stankewitz A, Aderjan D, Eippert F, May A. Trigeminal nociceptive transmission in migraineurs predicts migraine attacks. J Neurosci 2011;31(6):1937-1943.

[48] Szot P, Miguelez C, White SS, Franklin A, Sikkema C, Wilkinson CW, Ugedo L, Raskind MA. A comprehensive analysis of the effect of DSP4 on the locus coeruleus noradrenergic system in the rat. Neuroscience 2010;166(1):279-291.

[49] Takano T, Tian GF, Peng W, Lou N, Lovatt D, Hansen AJ, Kasischke KA, Nedergaard M. Cortical spreading depression causes and coincides with tissue hypoxia. Nat Neurosci 2007;10(6):754-762.

[50] Tassorelli C, Joseph SA. Systemic nitroglycerin induces Fos immunoreactivity in brainstem and forebrain structures of the rat. Brain Res 1995;682(1-2):167-181.

[51] Ter Horst GJ, Meijler WJ, Korf J, Kemper RH. Trigeminal nociception-induced cerebral Fos expression in the conscious rat. Cephalalgia 2001;21(10):963-975.

[52] van den Maagdenberg AM, Pietrobon D, Pizzorusso T, Kaja S, Broos LA, Cesetti T, van de Ven RC, Tottene A, van der Kaa J, Plomp JJ, Frants RR, Ferrari MD. A Cacna1a knockin migraine mouse model with increased susceptibility to cortical spreading depression. Neuron 2004;41(5):701-710.

[53] Vila-Pueyo M, Goadsby PJ, Holland PR. Locus Coeruleus Noradranergic Projections Modulate Cortical Spreading Depression Thresholds in Rats. Cephalalgia 2017;37:1-2.

[54] Vila-Pueyo M, Strother L, Goadsby PJ, Holland PR. The Role of the Locus Coeruleus in Regulating Trigeminovascular Nociception. Cephalalgia 2016;36:152-152.

[55] Zamalloa T, Bailey CP, Pineda J. Glutamate-induced post-activation inhibition of locus coeruleus neurons is mediated by AMPA/kainate receptors and sodium-dependent potassium currents. Br J Pharmacol 2009;156(4):649-661.

LEGENDS

Figure 1. Acute lesion of the LC disrupts trigeminovascular activation in a preclinical migraine model. **(A)** Schematic representation of the experimental setup of the model of dural-evoked trigeminovascular activation. A bipolar stimulating electrode is placed over the middle meningeal artery (MMA) to induce nociceptive activation of trigeminal afferents that signal via the trigeminal ganglion (TG) and innervate the dural vasculature, whilst projecting centrally to the trigeminocervical complex (TCC). A recording electrode placed in the TCC and a concentric bipolar tungsten electrode or a glass pipette placed in the locus coeruleus (LC) allow for recording and lesion/microinjection respectively. **(B)** An example TCC response showing neuronal activation (in grey) to dural stimulation (dashed line). **(C)** Time course changes in the average response of dural-evoked Aδ-fiber trigeminal neurons after placement of an electrode in the LC (control) or electrolytic lesion of the LC. Placement of an electrode in the LC (n = 6) induced a non-significant decrease in dural-evoked nociceptive neuronal activation in the trigeminocervical complex (TCC) (white bars). Subsequent electrolytic lesioning of the LC (n = 6) induced a significant decrease in dural-evoked neuronal activation in the TCC when compared to control (30min: $t_{(5)} = 2.76$, $p = 0.04$; at 60 min: $t_{(5)} = 3.24$, $p = 0.023$, grey bars) (AMP, amplitude; C1, first cervical level. Data are expressed as mean ± SEM, *$p < 0.05$).

Figure 2. DSP-4 treatment chronically disrupts LC noradrenergic projections and inhibits trigeminovascular activation. (A) Dopamine-β-hydroxylase (DBH) immunofluorescence in the locus coeruleus (LC) in saline and DSP-4 treated animals (white scale bar = 100 µm, white outlines were extracted from rat brain atlas [38]). **(B)** Percentage change in LC area immunoreactive for DBH in saline (n = 25, grey box) and DSP-4 (n = 25, black box) treated animals normalized to controls. DSP-4 treatment induced a significant loss of noradrenergic cells in the LC to 54 ± 5% compared to saline treated animals ($t_{(48)} = 6.32$, $p < 0.001$) (Data are expressed as median and interquartile ranges ***$p = 0.000027$). **(C)**

Schematic representation of the experimental setup of nociceptive trigeminovascular activation as a model of migraine-related pain processing. A bipolar stimulating electrode was placed over the superior sagittal sinus (SSS) to induce dural-evoked activation of trigeminal afferents from the trigeminal ganglion (TG) that innervate the dural vasculature. Neuronal activation was analysed by c-Fos immunohistochemistry detection within the trigeminocervical complex (TCC). **(D)** Photomicrographs showing c-Fos immunohistochemistry expression in the TCC in a representative animal of each experimental group. **(E)** Number of c-Fos immunoreactive positive cells in the TCC (n = 6 / group). Electrical stimulation induced a four-fold increase in neuronal activation in the TCC compared to sham in saline treated rats (U = 0, p = 0.006). However, in DSP-4 treated rats there was no difference in neuronal activation between sham and stimulated animals (U = 7, p = 0.144) (Data are expressed as median and interquartile ranges, black scale bar = 200 µm, **p = 0.006). 4V = 4th ventricle, DBHir = area immunoreactive for DBH, ir = immunoreactive, STIM = electrically stimulated.

Figure 3. Trigeminovascular activation is modulated by LC adrenoceptors. Time course changes in the average response of dural-evoked Aδ-fiber trigeminal neurons after microinjections in the locus coeruleus (LC). **(A)** Microinjection of the α2-adrenoceptor agonist clonidine induced a concentration-dependent reduction of the dural-evoked neuronal activation in the TCC when compared to the vehicle control group ($F_{4.45,66.8}$ = 12.96, p < 0.0001), reaching a significant decrease at 30 minutes after injection of the lowest concentration (1mg/ml, $t_{(12)}$ = -2.72, p = 0.019) and at 5 minutes after injection of the highest concentration (10mg/ml, $t_{(9)}$ = -7.56, p < 0.001). Pre-treatment with the α2-adrenoceptor antagonist yohimbine blocked the inhibitory effect ($F_{11,77}$ = 0.88, p = 0.561). **(B)** Microinjection of the α2-adrenoceptor antagonist yohimbine alone had no significant effect on dural-evoked trigeminovascular activation in the TCC when compared to the vehicle control group ($F_{11,110}$ = 0.44, p = 0.94). **(C)** Microinjection of α1-adrenoceptor agonist phenylephrine in the LC induced a biphasic response in dural-evoked activation in

the TCC. This response was characterised by an initial significant reduction of the neuronal activation to 81 % ± 5 that lasted 15 minutes (at 5 min: $t_{(10)} = -2.61$, $p = 0.026$; at 15 min: $t_{(10)} = -2.54$, $p = 0.029$), followed by a significant increase, reaching its maximum of 118% ± 8 at 60 minutes post injection ($t_{(10)} = 3$, $p = 0.013$). (Data are expressed as mean ± SEM, *p < 0.05).

Figure 4. Chronic disruption of the LC increases susceptibility to cortical spreading depression (CSD). (A) The electrical threshold (measured as the current intensity times stimulus duration; microCoulombs (μC)) to induce a CSD was significantly lower in the animals with their LC disrupted ($U = 43$, $p = 0.036$) indicating an increased susceptibility to CSD (Data are expressed as median and interquartile range in a logarithmic scale, *$p < 0.05$). *In vivo* cortical DC shift readings in a LC-intact **(B)** and a LC-disrupted **(C)** representative animal showing the application of increasing electric charges until a CSD was achieved. **(D)** Schematic representation of the experimental setup of CSD as a preclinical model of migraine aura. The electrical threshold to develop a CSD was determined on the left hemisphere by stimulating with a bipolar electrode increasing the electric charge. Once a CSD was induced, the number of KCl-induced CSDs was determined on the right hemisphere by placing a cotton ball soaked in 1M KCl. **(E)** The number of KCl-induced CSDs was significantly higher in the animals with their LC disrupted ($t_{(23)} = -2.5$, $p = 0.018$) confirming an increased susceptibility to CSD (Data are expressed as mean ± SEM). *In vivo* cortical direct current (DC)-shift readings in a LC-intact **(F)** and a LC-disrupted **(G)** representative animal showing the application of a cotton ball soaked in 1M KCl on the cortex surface (which was refreshed with 5μl every 15 minutes, black circles) inducing multiple CSDs throughout the 1-hour recording.

Figure 5: The locus coeruleus and migraine. The noradrenergic system plays a crucial role in the regulation of arousal and nociception. As one of the major sources of noradrenaline in the central

nervous system we sought to determine the role of the locus coeruleus (LC) in migraine pathophysiology. **(A)** Trigeminal nociceptive input from the head is conveyed via primary afferents arising in the trigeminal ganglion (TG) that synapse centrally on the trigeminocervical complex (TCC). From the TCC, ascending projections largely target the sensory thalamic nuclei; however, excitatory projections also target the LC resulting in its activation. During wakefulness, the LC receives descending excitatory projections from the hypothalamus that promote its activation (green arrow). In turn, the LC sends noradrenergic projections to most of the CNS, including descending projections to the TCC and spinal cord, as well as ascending projections to the thalamus and cortex, having roles in arousal and nociceptive processing. **(B)** We have demonstrated that loss of LC noradrenergic signalling inhibits trigeminal nociceptive signalling at the level of the TCC, while paradoxically increasing the susceptibility to cortical spreading depression (CSD). As such, we propose that inhibition of the LC exerts a potent anti-nociceptive effect on trigeminal nociceptive processing. As the LC shows diurnal activity, falling almost completely silent during, sleep we further hypothesise that sleep-induced LC inhibition may be a potential mechanism.

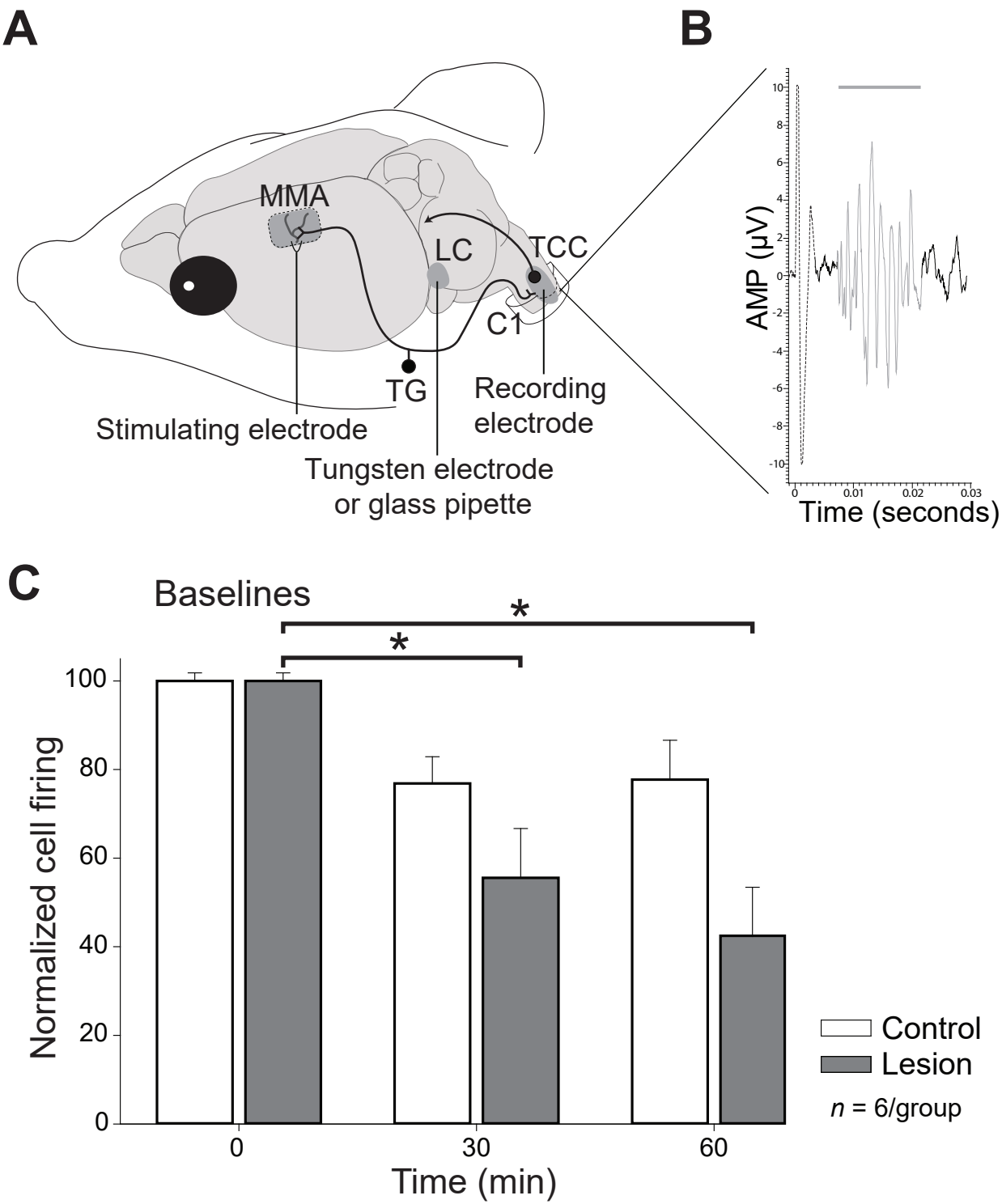
A
MMA
LC
TCC
C1
TG
Recording electrode
Stimulating electrode
Tungsten electrode or glass pipette
B
AMP (μV)
Time (seconds)
C
Baselines
*
*
Normalized cell firing
Time (min)
Control
Lesion
n = 6/group

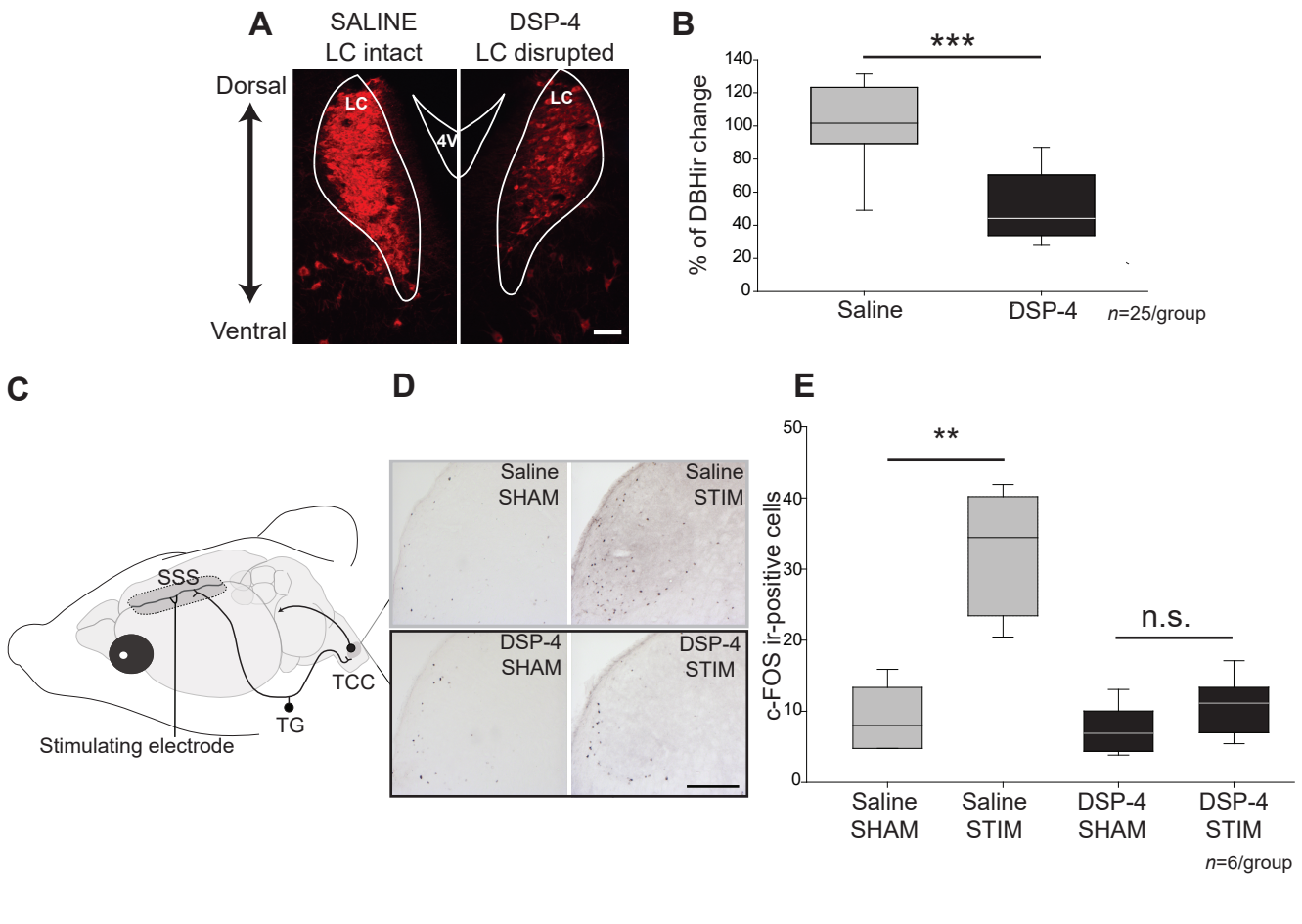
A
SALINE
LC intact
DSP-4
LC disrupted
Dorsal
Ventral
LC
4V
LC
B
***
% of DBHir change
140
120
100
80
60
40
20
0
Saline
DSP-4
n=25/group
C
SSS
TCC
TG
Stimulating electrode
D
Saline
SHAM
Saline
STIM
DSP-4
SHAM
DSP-4
STIM
E
**
n.s.
c-FOS ir-positive cells
50
40
30
20
10
0
Saline
SHAM
Saline
STIM
DSP-4
SHAM
DSP-4
STIM
n=6/group

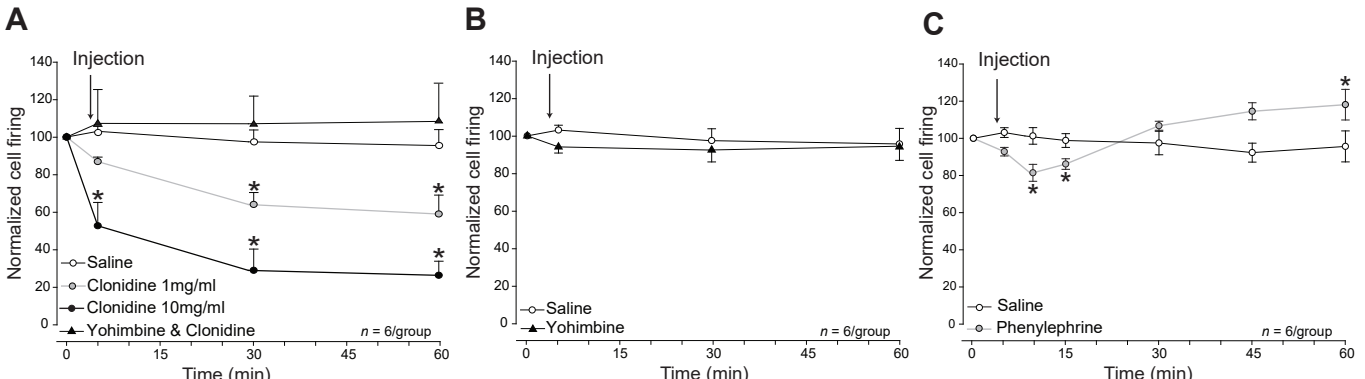
A
Injection
Normalized cell firing
Time (min)
Saline
Clonidine 1mg/ml
Clonidine 10mg/ml
Yohimbine & Clonidine
n = 6/group
B
Injection
Normalized cell firing
Time (min)
Saline
Yohimbine
n = 6/group
C
Injection
Normalized cell firing
Time (min)
Saline
Phenylephrine
n = 6/group

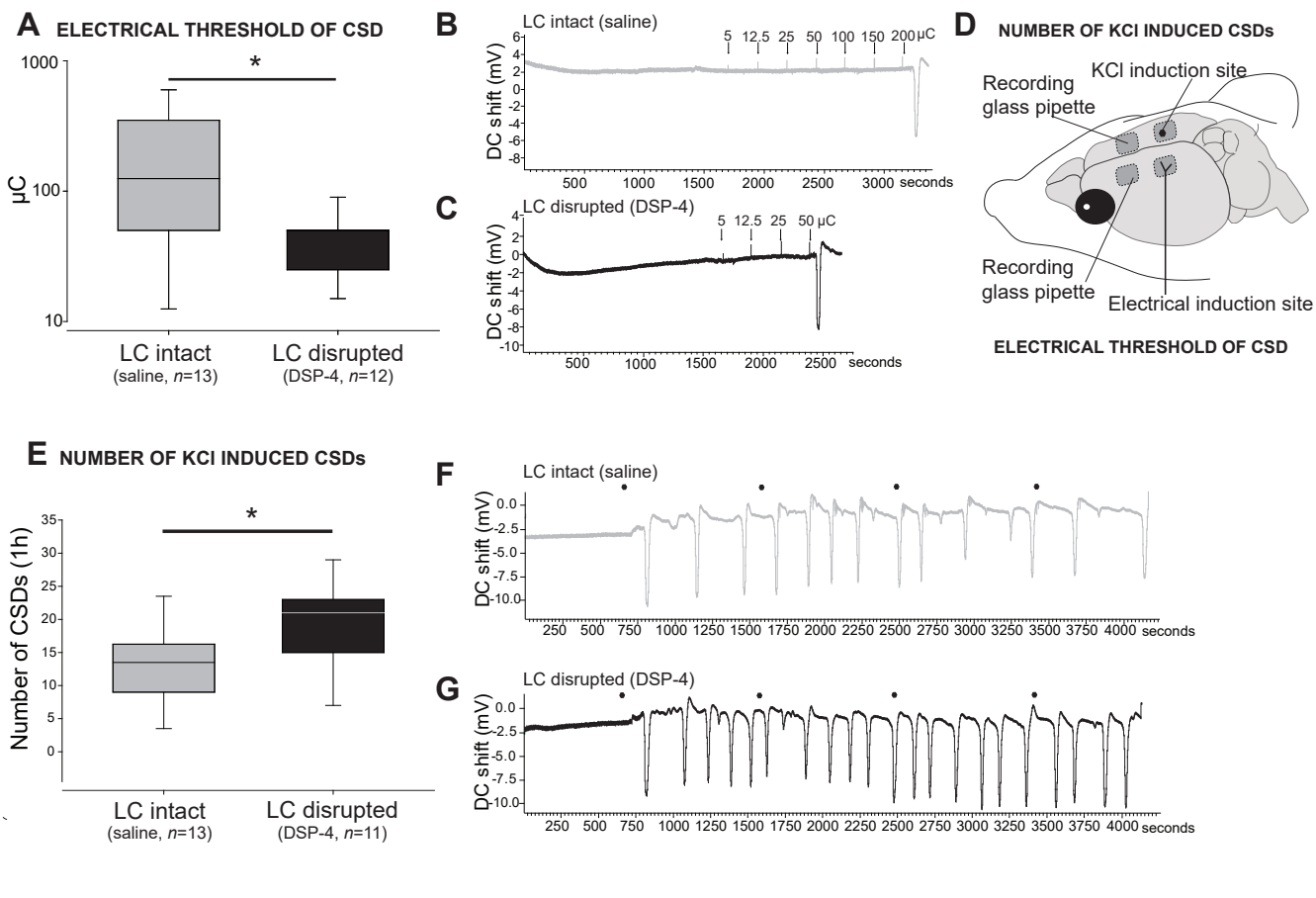
A
ELECTRICAL THRESHOLD OF CSD
1000
100
10
µC
*
LC intact
(saline, n=13)
LC disrupted
(DSP-4, n=12)
B
LC intact (saline)
5 12.5 25 50 100 150 200 µC
DC shift (mV)
seconds
C
LC disrupted (DSP-4)
5 12.5 25 50 µC
DC shift (mV)
seconds
D
NUMBER OF KCl INDUCED CSDs
Recording glass pipette
KCl induction site
Recording glass pipette
Electrical induction site
ELECTRICAL THRESHOLD OF CSD
E
NUMBER OF KCl INDUCED CSDs
Number of CSDs (1h)
*
LC intact
(saline, n=13)
LC disrupted
(DSP-4, n=11)
F
LC intact (saline)
DC shift (mV)
seconds
G
LC disrupted (DSP-4)
DC shift (mV)
seconds

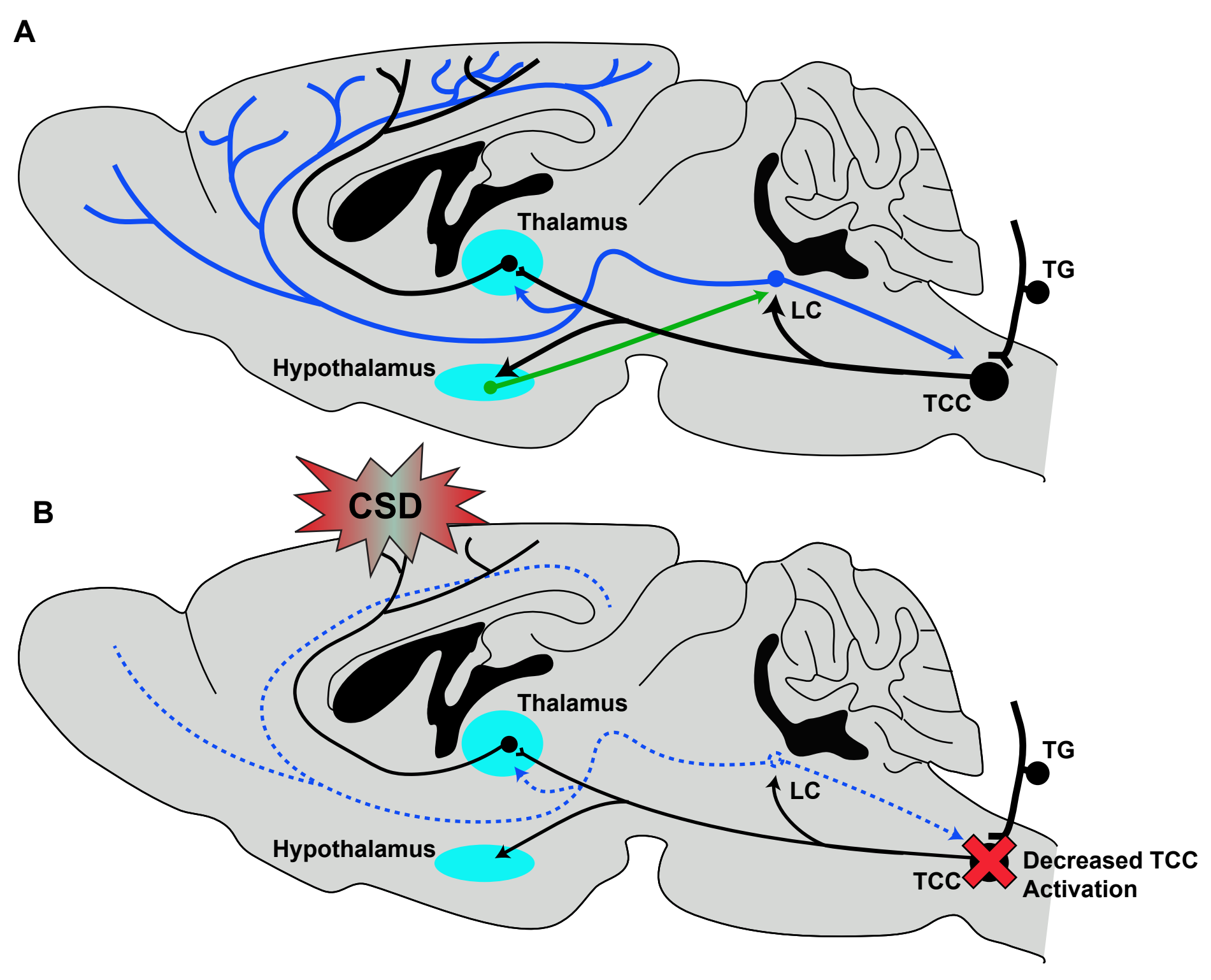
A
Thalamus
TG
LC
Hypothalamus
TCC
B
CSD
Thalamus
TG
LC
Hypothalamus
TCC
Decreased TCC
Activation

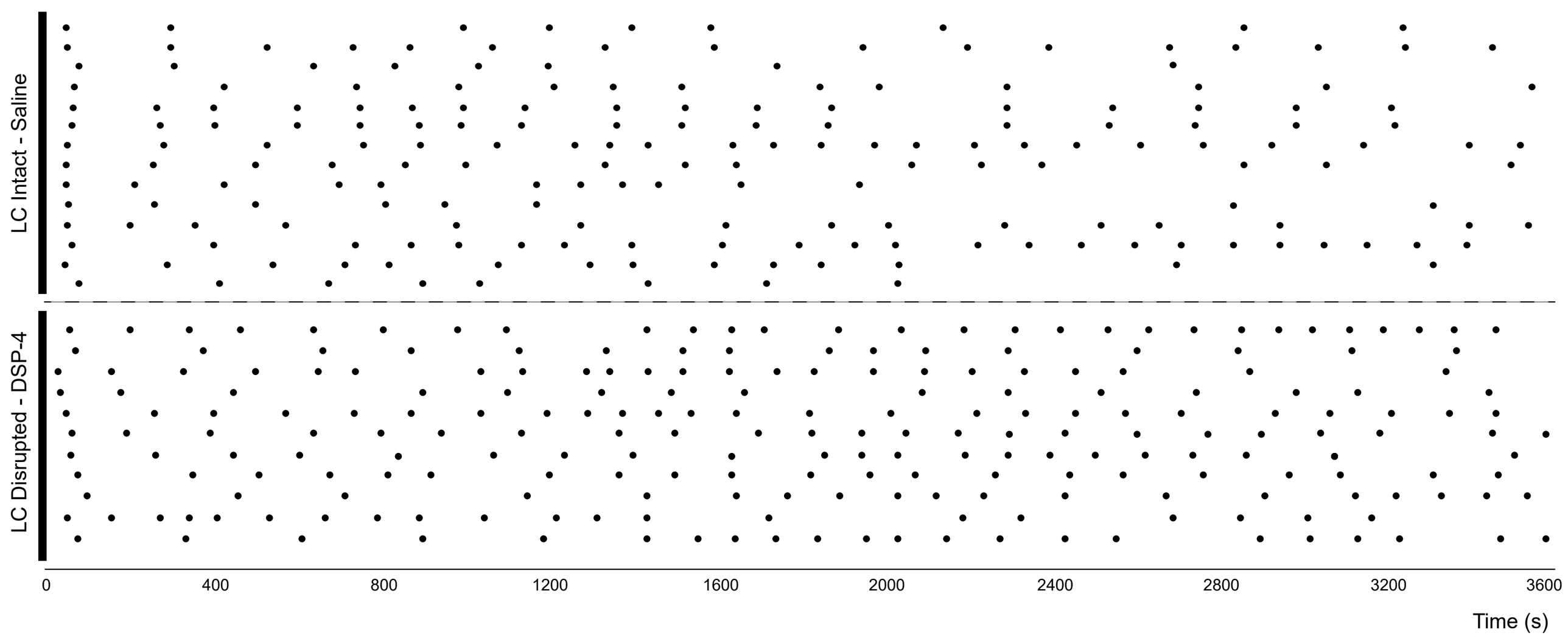
LC Intact - Saline
LC Disrupted - DSP-4
0
400
800
1200
1600
2000
2400
2800
3200
3600
Time (s)